

The Eurasia Proceedings of Science, Technology, Engineering and Mathematics (EPSTEM), 2025

Volume 37, Pages 359-373

**ICEAT 2025: International Conference on Engineering and Advanced Technology**

## Experimental Investigation of Energy Performance in Double-Glazed Windows Utilizing Air and Phase Change Materials

**Mai AbdulKhaleq Abd-Oun**  
University of Al-Qadisiyah

**Alaa Liaq Hashem**  
University of Al-Qadisiyah

**Ahmed AbdelKadhem Majhool**  
University of Al-Qadisiyah

**Abstract:** The growing emphasis on energy efficiency in buildings necessitates advancements in building envelope components, particularly windows, which significantly influence thermal comfort and energy consumption. This study experimentally evaluates the thermal performance of double-glazed windows incorporating paraffin wax phase change material (PCM) versus traditional air-filled cavities, aiming to enhance energy efficiency in buildings under varying solar radiation intensities. A modular insulated chamber (1 m<sup>3</sup> PVC structure) with a double-glazed window opening was subjected to controlled radiant loads (500 and 1000 W/m<sup>2</sup>). Two 9mm-cavity configurations were tested: one filled with air and another with paraffin wax PCM (melting range: 56–58°C). Temperatures and heat flux were monitored using thermocouples and a data logger. PCM reduced cumulative heat transfer by 22% at 500 W/m<sup>2</sup> and 35% at 1000 W/m<sup>2</sup> compared to air. At 1000 W/m<sup>2</sup>, PCM delayed peak thermal loads by 2.67 hours and reduced glass surface temperature gradients ( $\Delta T$ ) by 20.4%. Under 500 W/m<sup>2</sup>, PCM increased peak heat flux by 15% due to solid-state conduction but still lowered cumulative energy transfer by 22% via thermal mass enhancement. PCM significantly improves thermal buffering and energy efficiency in double-glazed windows under high solar irradiance ( $\geq 1000$  W/m<sup>2</sup>), reducing HVAC reliance. Optimal performance requires radiation sufficient to activate phase change (56–58°C), validating PCM's suitability for high-solar regions.

**Keywords:** PCM, Double-glazed windows, Building insulation, Thermal lag, Paraffin packaging, Solar heat gain control.

### Introduction

The building sector is a major energy consumer, responsible for approximately 40% of the world's total energy use. This high consumption is largely driven by the operational demands of heating, cooling, lighting, and ventilation systems. Enhancing energy efficiency represents a critical strategy for mitigating climate change and addressing escalating energy expenditures and carbon emissions (Gaur et al., 2019). Within this framework, the building envelope, with windows being a pivotal element, plays an essential role in optimizing the balance between occupant thermal comfort and overall energy performance. Windows act as the primary barrier regulating heat exchange between a building's interior and the external environment, directly controlling heat loss during winter and solar heat gain during summer. Insufficient thermal resistance in these components leads to increased reliance on heating, ventilation, and air conditioning (HVAC) systems, underscoring the necessity for advanced technological solutions. Although double-glazed windows are widely implemented for their superior insulating properties, their documented limitations in achieving maximum energy conservation and managing thermal fluctuations remain a significant challenge (Filippín, 2007). Numerical study using ANSYS Fluent, to increasing

- This is an Open Access article distributed under the terms of the Creative Commons Attribution-Noncommercial 4.0 Unported License, permitting all non-commercial use, distribution, and reproduction in any medium, provided the original work is properly cited.

- Selection and peer-review under responsibility of the Organizing Committee of the Conference

air gap thickness improves thermal efficiency until reaching the optimal thickness (14 mm for air). Air reduced heat transfer by 86.9% compared to single-glazed windows. Moreover, a study conducted a numerical investigation of the impact of window characteristics on the thermal performance of double-glazed windows in Libya's climatic zone. The thickness of the window's gas space, gas filling (air and argon were tested and compared), and frame material (U-PVC, wood, and aluminum) were all investigated. The results reveal that raising the gas spacing thickness improves the window's thermal efficiency.

While a numerical approach to analyzing the thermal performance of single and double-glazed windows in Libyan climate (Mitiga Airport), 14 mm air gap (13 mm for argon) achieves optimal thermal performance with minimal heat loss. (Alharari et al., 2023), while; Experimental and CFD simulation study, the dual airflow window improved heat recovery efficiency (20-56%) and increased winter performance by up to 20% using captured solar energy. Risk of condensation in humid conditions was noted, optimal cavity width of 9 mm maximizes heat recovery efficiency (Gosselin & Chen, 2008).

However, the impact of pine wood waste panels used in window frames and double-glazing systems on the energy demand for heating, cooling, and artificial lighting in a typical 1970s residential building under various climate conditions. Scraps from breakthrough transparent glazing systems make eco-sustainable panels with natural flour-based adhesive. Air gaps with insulating panels reduced U-values by 65–67%, enhancing building energy efficiency (Merli & Buratti, 2024). Numerical simulation via computational fluid dynamics (CFD) is used to evaluate and optimize advanced window assemblies, including modified air supply windows. This methodology has yielded U-values low as  $0.1\text{--}0.5\text{ W/m}^2\text{ K}$ , demonstrating performance significantly exceeding that of three-pane glass (Gloriant et al., 2015). However, the predictive reliability of these simplified models is often limited, as their basic boundary conditions can overlook 3D geometric complexities and thermal bridging through window frames.

At the same time, high-performance glazing systems, such as those incorporating airgel or vacuum insulation panels, achieve remarkable thermal performance ( $U=0.28\text{ W/m}^2\cdot\text{K}$ ) but face significant costs, making traditional double or triple glazing more viable for wider implementation (Michael et al., 2023). Double-flow windows, calibrated for an air flow rate of 10 l/s and cavity depth of 9 mm, show expected heat recovery efficiencies of 20% to 56%, albeit necessitating the implementation of condensation control measures (Gosselin & Chen, 2008). In an investigation related to these developments, Hariri et al. (2023) studied the thermal performance of single- and double-glazing units in the Libyan climate using a 2D numerical model in ANSYS Fluent software. Their findings revealed that argon-filled double glazing reduces heat transfer by 90.5% compared to single glazing, setting an ideal cavity width of 14 mm for argon gas. Based on this research, a double-glazed unit featuring a dual airflow configuration was developed and its performance was enhanced through an integrated approach of CFD modeling and experimental field measurements. The optimal cavity width was found to be 9mm, achieving a thermal recovery efficiency of 56%, which reduces energy consumption in cold regions. (Gosselin & and Chen, 2008)

Recycled wooden panels were integrated into double-glazing with air gap. Experimental analysis and dynamic simulations demonstrated an 11% reduction in cooling consumption in hot climates like Rome (Merli & Buratti, 2024). While simplified models were developed to simulate ventilated double-glazing, showing an effective U-value of  $0.1\text{ W/m}^2\cdot\text{^\circ C}$  and an 80% reduction in heat loss compared to traditional triple glazing (Gloriant et al., 2015). A numerical model was developed to simulate the performance of exhaust air double glazing in mixed climates, and the results showed an energy saving of 38.2%. The results revealed superior performance compared to mechanical ventilation with heat recovery (MVHR) systems during cold seasons (Guo & Zhang, 2022).

Contemporary research focuses on incorporating phase change materials (PCMs) and nanoparticle-enhanced PCMs into the cavities between glass panels. These materials—such as paraffin-based composites reinforced with silica ( $\text{SiO}_2$ ) or titanium ( $\text{TiO}_2$ ) nanoparticles (Cieslinski et al., 2023; Marhoon et al., 2024)—leverage their ability to store latent heat during phase transitions to regulate internal temperatures, thus reducing energy demand. Studies show that PCM-integrated windows can reduce cooling energy consumption by up to 46% in climates with large diurnal temperature variations (Nsaif et al., 2023). However, the effectiveness of these systems is contingent on climate-specific design and nanoparticle stability, highlighting the need for further research on long-term performance (D'Oliveira et al., 2022).

Furthermore, a thermal model of PCM-filled double glazing is developed and experimentally validated, demonstrating accurate simulation of heat transfer during the phase transition under solar radiation. The effect of PCM optical properties (particularly the extinction coefficient) on the thermal performance was analyzed. The results showed that increasing the modulus from 5 to 200 sccm accelerates the heat absorption in solid PCM by 300 min (Li et al., 2016). In a related study, enhancing the absorption coefficient of glass to  $160\text{ m}^{-3}$  improved

energy efficiency by 41.53% in northern China (Wang et al., 2023). A 2D model optimized PCM performance by adding nanoparticles like  $\text{TiO}_2$ , reducing summer indoor temperatures by 0.82 but increasing winter heating needs (Zhang et al., 2020).

Table 1. Comprehensive summary of prior research on advanced glazing systems.

Year	Author(s)	Parameters Studied	Study Type	Enhancement Method	Key Findings
2008	Gosselin and Chen, (2008)	Cavity width, airflow rates	Experimental + CFD	Dual airflow window	20-56% heat recovery efficiency; 20% winter performance boost; optimal cavity width = 9 mm
2010	Mahlia and Iqbal (2010)	Insulation thickness, air gaps	Cost-benefit analysis	Optimal insulation + air gaps	Identified economic thickness thresholds; emission reduction potential
2015	Gloriant et al. (2015)	Triple-glazed ventilation	Numerical modeling	Supply-air triple glazing	U-value = 0.1–0.5 W/m <sup>2</sup> K; 80% heat loss reduction vs. triple glazing
2015	Goia et al. (2015)	Optical properties of PCM	Experimental	PCM-filled double glazing	Measured spectral properties (error <4%); validated angular solar characteristics
2016	Liu et al. (2016)	PCM phase change dynamics	Numerical + Experimental	Non-ventilated PCM double glazing	Model accurately predicted heat transfer during phase change under solar radiation
2016	Li et al. (2016)	PCM extinction coefficient (5–200 m <sup>-1</sup> )	Numerical	Optical property optimization	Heat absorption accelerated by 300 min with higher extinction coefficients
2020	Zhang et al. (2020)	TiO <sub>2</sub> nanoparticles in paraffin PCM	2D Numerical model	Nano-enhanced PCM glazing	Summer indoor temp ↓0.82°C; slight winter heating penalty
2022	Guo and Zhang (2022)	Exhaust-air heat recovery	Numerical	Double exhaust-air glazing	38.2% energy savings in mixed climates; outperformed MVHR systems in winter
2023	Huang et al. (2023)	PCM thickness, frame integration	Experimental	Thick supply-air window with PCM cavity-frame	Quantified thermal buffering effects in practical window assemblies
2023	Wang et al. (2023)	Glass absorption coefficient (≤160 m <sup>-1</sup> )	Statistical analysis	PCM + solar control glass	↑41.53% energy efficiency in northern China with optimized absorption
2023	Lu et al. 2023	Climate zones, PCM layer configuration	Numerical optimization	Multilayer PCM glazing	Climate-specific optimal structures identified for energy savings
2023	Alharari et al. (2023)	Air and Argon-filled double glazing	Numerical simulation	Air and Argon-filled double glazing	Argon-filled windows reduced heat transfer by 90.5%, and air-filled by 86.9%. The optimal gap spacing was 14mm for air and 13mm for argon
2024	Merli and Buratti, (2024)	Wood waste panels, U-values	Experimental + Simulation	Recycled wood panels in double glazing	U-values ↓65–67%; cooling consumption ↓11% in hot climates
2024	Nsaif et al. (2024)	Triple glazing, Iraqi climate	Numerical	Paraffin wax PCM in triple glazing	TW-PCM reduced internal surface temperatures by 3.1°C and delayed peak heat loads by 2 hours, improving thermal performance.

The optical properties of paraffin layers in double-glazing were measured using a 75cm integrating sphere, with a relative measurement error below 4%. (Goia et al., 2015), Triple-glazed paraffin-filled windows were analyzed in Iraq's climate, showing a 2-hour delay in peak heat and a 3.1°C reduction in indoor temperatures compared to traditional windows. (Nsai et al., 2024), and also, While Effective thermal insulation with a 2-hour delay in peak heat, though optical clarity requires design optimization. While, Materials like  $\text{Na}_2\text{SO}_4 \cdot 10\text{H}_2\text{O}$  enhance summer thermal regulation but fail in winter due to mismatched melting points. (Liu et al., 2016). Despite progress, critical gaps remain. Improved phase change material (PCM) optimizations for extreme climates, nanoparticle concentration thresholds (<5% for paraffin; (Marhoon et al., 2024)), and hybrid designs that integrate multiple technologies (e.g., low-emissivity coatings with aerogel layers) have yet to be explored (Lu et al., 2023). Table 1 gives a comprehensive summary of prior research on advanced glazing systems. While existing research demonstrates the theoretical potential of PCMs, this study contributes to filling critical gaps by experimentally measuring paraffin wax PCMs in double glazing compared to standard air-filled modules under controlled radiant loads (500/1000  $\text{W/m}^2$ ), and uniquely tests (a) irradiance-dependent efficiency gains and (b) phase-change-induced thermal lag as a design metric. This work contributes to the development of sustainable building practices through tailor-made, high-performance window solutions.

## Theoretical Background

### Composite Wall

In accordance with Fourier's law of heat conduction, the thermal energy flux ( $Q$ ), measured in watts ( $\text{W}$ ), and arises within wall assemblies due to the absorption of incident radiation at the exterior surface. This flux is directly proportional to:

- i. The thermal gradient ( $\Delta T$ ) across the wall, measured in °C.
- ii. The material-specific thermal conductivity ( $k$ ), expressed in  $\text{W/m} \cdot ^\circ\text{C}$ .
- iii. The cross-sectional area ( $A$ ), measured in  $\text{m}^2$ .

Conversely, it is inversely proportional to the layer thickness ( $x$ ), measured in meters, as articulated in Equation (1):

$$Q = -k \times A \times dT/dx \quad 1$$

In multilayer or composite wall systems, materials with differing thermal conductivities (e.g., PCM-enhanced layers or insulation) are combined, discontinuities in the thermal gradient occur at the interfaces between materials. For these systems, the cumulative thermal resistance, which accounts for both conductive and convective effects, governs the net heat transfer. The generalized heat flux equation (Equation(3)) incorporates the overall heat transfer coefficient ( $U$ ), measured in  $\text{W/m}^2 \cdot ^\circ\text{C}$ , which quantifies the combined resistance of all layers (Alaa Abdulhussein & Hashem, 2021).

$$Q = U \times A \times \Delta T \quad 2$$

This theoretical framework is critical for analyzing the energy performance of advanced glazing systems, such as the double-glazed windows with PCM, air cavities studied in this work. For instance:

*PCM Integration:* Phase-change materials introduce variable thermal conductivity during phase transitions, dynamically altering the  $U$ -value and delaying heat penetration. Equation 3 calculates the specific heat at these different states of PCM.

$$(\rho C)_{PCM} = \begin{cases} \frac{(\rho C)_{solid} + (\rho C)_{liquid}}{2} + \frac{\rho_{solid} + \rho_{liquid}}{2} \left( \frac{\lambda}{\Delta T} \right) & T < T_{solid} \\ (\rho C)_{liquid} & T_{solid} \leq T \leq T_{liquid} \\ & T > T_{liquid} \end{cases} \quad 3$$

Where:  $\Delta T = T_{liquid} - T_{solid}$

The term  $(\rho)$  refers to the density in ( $\text{Kg/m}^3$ ) units.  $T_{liquid}$  ( $^\circ\text{C}$ ) is the temperature at which the paraffin melt.  $T_{solid}$  ( $^\circ\text{C}$ ) is the temperature at which paraffin solidifies,  $\lambda$  refers to latent heat of fusion which is different for each

material. When using PCM as part of the wall layers, equation (4) demonstrates the amount of flux that move through the wall. Where  $Q_{stored}$  is equal to the heat stored in the phase change material.

$$Q_{cond} = Q_{flux} - Q_{stored} \text{ (W)}$$

4

*Air Cavities:* Air gaps eliminate conductive/convective losses, minimizing  $\Delta T$  across the cavity and elevating the system's effective U-factor. By applying Equations (1-4) the study quantifies how these material innovations modulate heat flux under varying radiative loads (500–1000 W/m<sup>2</sup>), providing a thermodynamic basis for comparing energy efficiency in building envelopes.

Temperature and heat flow reductions are calculated from experimental data using the equations below.

$$\text{Temperature reduction} = (1 - \frac{\Delta T_{PCM}}{\Delta T_{air}}) \times 100\% \quad 5$$

$$\text{Heat flow reduction} = (1 - \frac{Q_{PCM}}{Q_{air}}) \times 100\% \quad 6$$

Where:  $\Delta T$  is the temperature difference (°C) between external and internal surfaces of double-glazed windows under specified radiation conditions, measured for both PCM-filled and air-filled cavity configurations.  $Q$  represents the internal heat flux (W/m<sup>2</sup>) through double-glazed windows under specified radiation conditions, evaluated for both PCM and air gap implementations.

## Materials and Methods

### Model Configurations

Cube-shaped structure with dimensions of 1m × 1m × 1m was constructed using PVC material for the main body frame, while the outer frame surfaces was made of PVC panels (thickness: 15 mm) with thermal conductivity 0.28 W/m·K minimized conductive losses and to ensure durability and lightweight properties, as illustrated in Figure (1). The thermodynamic properties of the materials utilized in the fabrication of the model are presented in Table 2. ASHRA (2017) and ASM (1990)

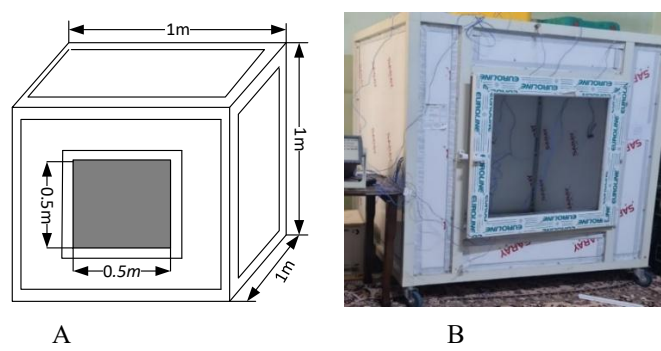


Figure 1. a) Schematic design and b) physical prototype of the experimental chamber.

Table 2. Thermo-physical properties of wall construction materials

Materials	Conductivity (W/m.K)	Specific heat (J/kg.K)	Density (kg/m <sup>3</sup> )
Air	0.026	1005	1.2
Glass	1.38	840	2300
PVC	0.28	1170	1380

### Window Double Glazed Samples

Two samples of double-glazed windows were designed to investigate the effectiveness of phase change materials (PCMs) in enhancing thermal insulation. Two of the samples featured a 9mm interstitial gap between the glass

layers, with one filled with air and the other containing PCM. All samples were engineered to comply with technical standards, with gaps sealed using thermal silicone glue to prevent material leakage.

### Phase Change Material (PCM)

Paraffin wax, designated as PARAFFIN WAX PELLETS, was utilized as a latent heat storage material in this study, as illustrated in Figure 2. During the procedure, the wax is melted, and the necessary quantity is injected into the interstitial space between the two glass plates. The thermo-physical properties of paraffin wax are presented in Table 3. (Loba Chemie)

Table 3. Thermo-physical properties of Paraffin wax-based on PCM.

Property	Values
Melting temperature range	56-58°C
Heat storage capacity	174 kJ/kg
Specific heats in both solid and liquid	2 kJ kg <sup>-1</sup> K <sup>-1</sup>
Density in solid state	880 kgm <sup>-3</sup>
Density in liquid state	760 kgm <sup>-3</sup>
Volume expansion (solid/liquid phase change)	16%
Thermal conductivity in both solid and liquid states	0.2Wm <sup>-1</sup> K <sup>-1</sup>



Figure 2. The paraffin wax packing.

Experiments were conducted in a laboratory environment with a constant indoor temperature of  $25 \pm 2^\circ\text{C}$  and a relative humidity of  $45 \pm 5\%$ . Closing the test window within the insulated chamber negated the effect of wind. Heat buildup was mitigated via the chamber's insulation (PVC) and controlled indoor laboratory temperature. This controlled setup isolated radiation intensity as the only external variable affecting thermal performance.

### Experimental Procedures

The following steps were implemented to fill the gap between double glass windowpanes with paraffin wax: as shown in Figure 3.

- 1- Melting Process: The paraffin wax was subjected to control heating to initiate the melting process.
- 2- Temperature Regulation: The temperature was elevated to  $60^\circ\text{C}$ , significantly surpassing the wax's melting range of  $56-58^\circ\text{C}$ . This ensured that the material remained in a liquid state throughout the filling procedure.
- 3- Syringe Injection: The molten wax was drawn into a syringe and subsequently injected into the cavity between the double glass panes through designated openings.



Figure 3. (a) Window with integrated PCM. (b) Injecting liquid PCM into the double-glazed cavity.

## Measuring Devices Utilized

A data logger (model AT45xx) equipped with a high-performance ARM microprocessor was employed to record temperature measurements over time. This device is compact, lightweight, and supports inputs from 16 temperature sensors. The system was configured to periodically record temperatures from the outer surface, the phase change material (PCM) layer, and the inner surface at 2-minute intervals. Type-K thermocouples were utilized for temperature sensing. The distribution of the thermocouples and the schematic diagram of the model are illustrated in Figures 4 and 5.

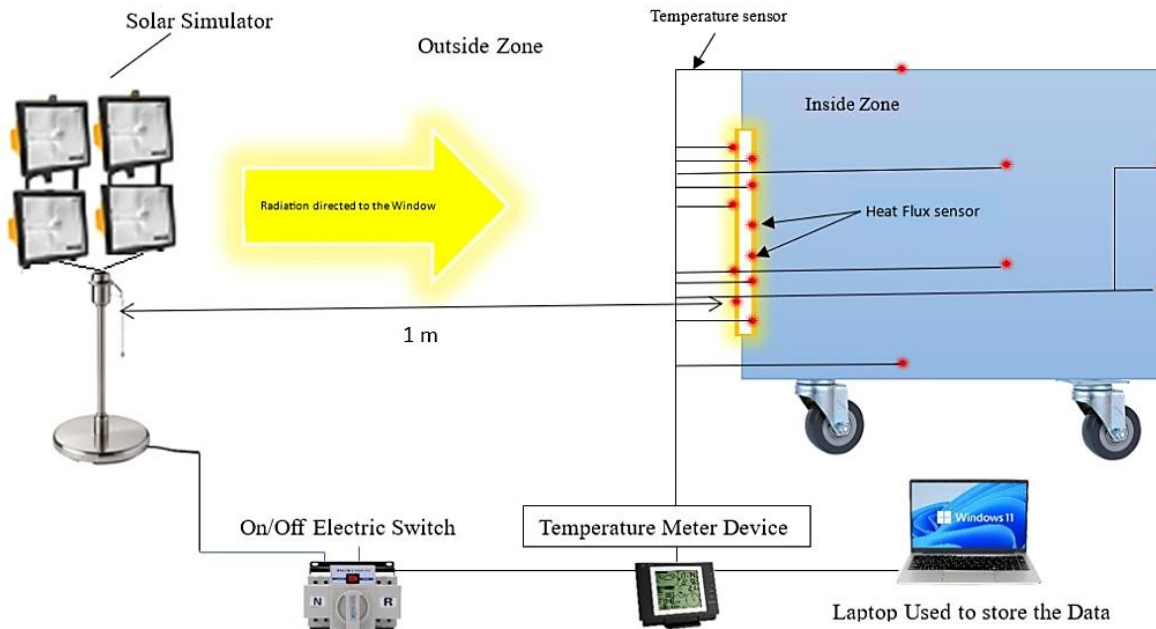


Figure 4. Schematic of indoor experimental setup and instrumentation.

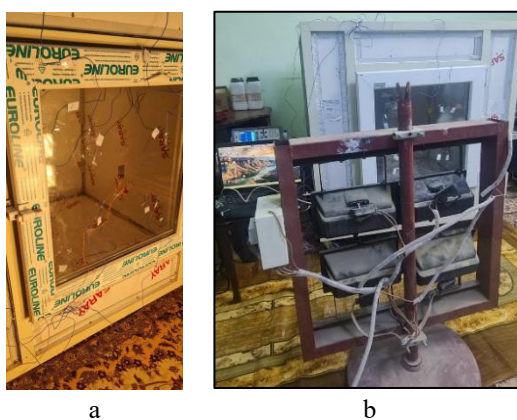


Figure 5. (a) Thermocouples installed on interior and exterior window surfaces.  
 (b) Setup showing solar simulator and dataloggers with the test chamber.

The K-type thermocouples were calibrated by testing them in water bath at standard reference temperatures (ice, room temperature, and boiling point), comparing their readings against a mercury thermometer. The observed error rates were acceptably low ( $\pm 0.05$ ). The heat flux sensor relied on the manufacturer's factory calibration accuracy 5% (FluxTeq).

## Results and Discussions

An experimental study evaluated three double-glazed window samples under two solar radiation conditions:  
*Case 1:* 500 W/m<sup>2</sup> constant radiation.

Case 2: 1000 W/m<sup>2</sup> radiation intensity.

Each sample was tested under both conditions:

1. *Air gap sample*: double glazed – sealed air gap.

2. *PCM gap sample*: double glass - gap filled with paraffin wax.

### Thermal Performance Analysis

#### Under 500 W/m<sup>2</sup> Radiation

*Air-gap sample*: In the air-gap sample, the temperature of the outer surface rose to 45 °C, as shown in Figure 6, while the temperature of the inner surface reached 43.8 °C within 2 hours of irradiation. This delay in heat transfer is due to the low thermal conductivity of the air (0.026 W/m.K).

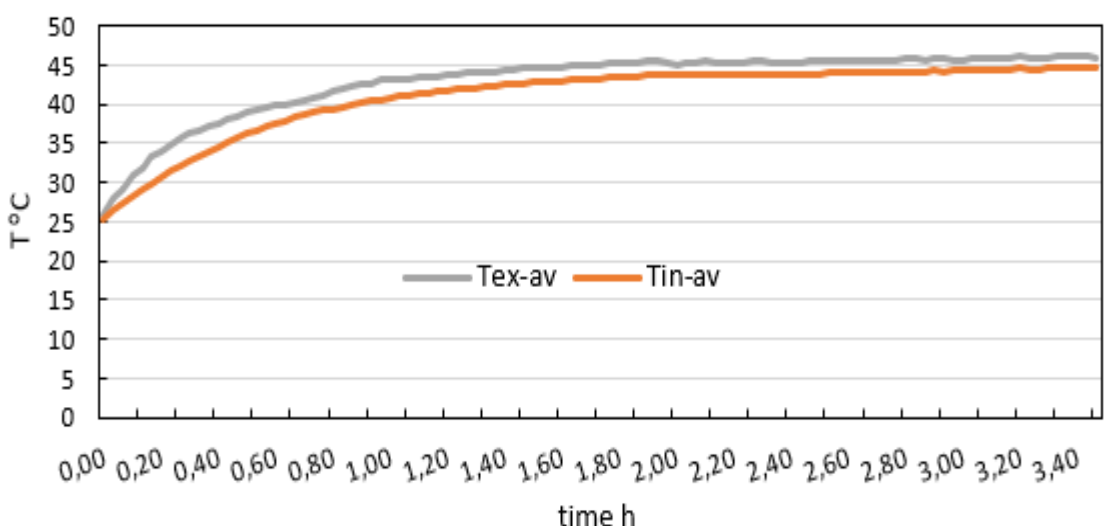


Figure 6. External and internal temperature for double glass window with 9mm air cavity under 500 W/m<sup>2</sup>

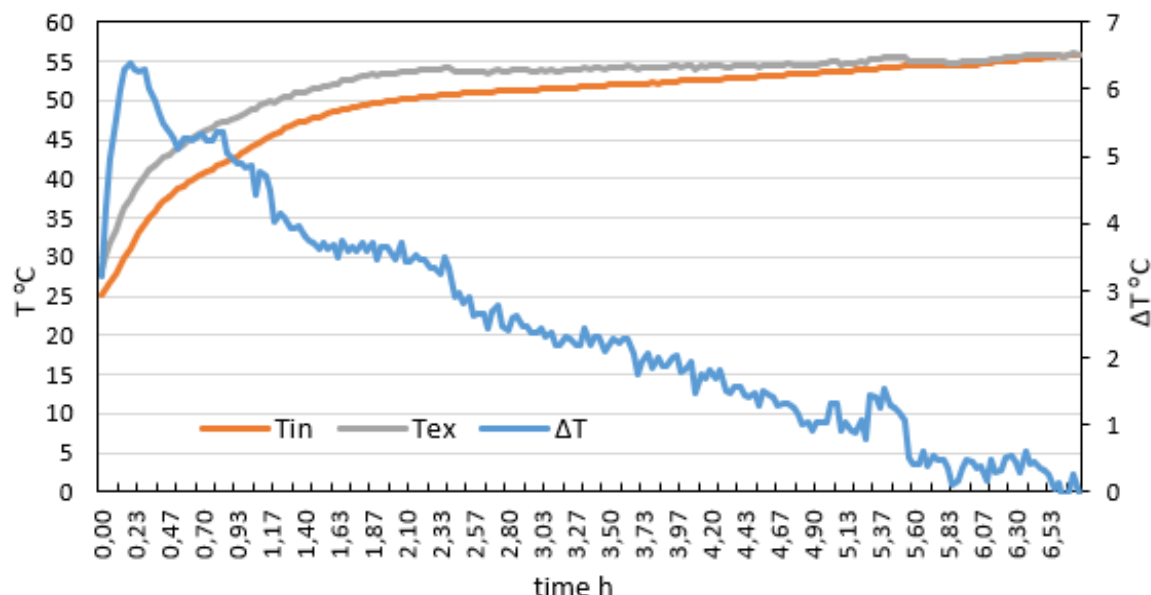


Figure 7. External, Internal and difference temperature for double glass window with 9mm cavity with PCM under 500 W/m<sup>2</sup>

*PCM sample*: The PCM sample recorded higher maximum temperature values compared to the air gap sample. The temperature of the inner cavity in the sample containing PCM reached 49.9°C after two hours of irradiation as shown in Figure 7, while the outer surface recorded 53.45°C. This slight thermal variation is due to the paraffin

not reaching the phase transition temperature range (56-58°C), which resulted in it remaining in the solid phase. This in turn allowed. The high thermal conductivity (0.2 W/m·K - Table 3) transfers thermal energy more efficiently than the air gap.

#### Under 1000 W/m<sup>2</sup> Radiation

*Air-gap sample:* Figure 8 demonstrates that despite the low thermal conductivity of air, the inner surface experiences a sharp temperature increase during the initial heating phase, reaching 56.55°C within the first hour. This behavior results from the substantial temperature differential between the outer surface (61.7°C) and the inner surface, creating a steep thermal gradient across the cavity. Following this initial surge, the rate of temperature increase diminishes significantly, stabilizing at 57.47°C after two hours as the system approaches thermal equilibrium.

*PCM sample:* Three distinct thermal response regions, governed by the phase behavior of the Phase Change Material (PCM) under a 1000 W/m<sup>2</sup> radiation intensity, can be identified in Figure 9.

#### Zone 1: Sensible Heating (T < 56°C)

During the first hour after the start of irradiation, the PCM remains below its melting point (56°C). The internal temperature rises sharply at a rate of approximately 8°C per hour due to the following reasons:

- Pure conductive heat transfer through solid paraffin ( $k_{\text{solid}} = 0.2 \text{ W/m}\cdot\text{K}$ ).
- No latent heat absorption ( $\lambda = 174 \text{ kJ/kg}$  not activated).
- High thermal driving force ( $\Delta T$ ).

#### 1. Zone 2: Phase Transition (56°C ≤ T ≤ 58°C)

From  $t=1\text{h}$  to  $t=1.77\text{h}$ , the outer surface exceeds 56°C, initiating melting. This suppresses the inner temperature rise to <2°C/hour because:

- Energy is diverted to latent heat absorption.
- Isothermal behavior dominates during phase change.

#### 2. Zone 3: Liquid Conduction (T > 58°C)

Beyond  $t=1.77\text{h}$ , fully liquid PCM exhibits accelerated heat transfer:

- Inner temperature rises at ~12°C/hour (vs. air's ~9°C/hour)
- Enhanced conduction through liquid paraffin ( $k_{\text{liquid}} = 0.2 \text{ W/m}\cdot\text{K}$  vs air's 0.026 W/m·K)
- Cumulative thermal lag reaches 1.5 hours due to phase-change delay.

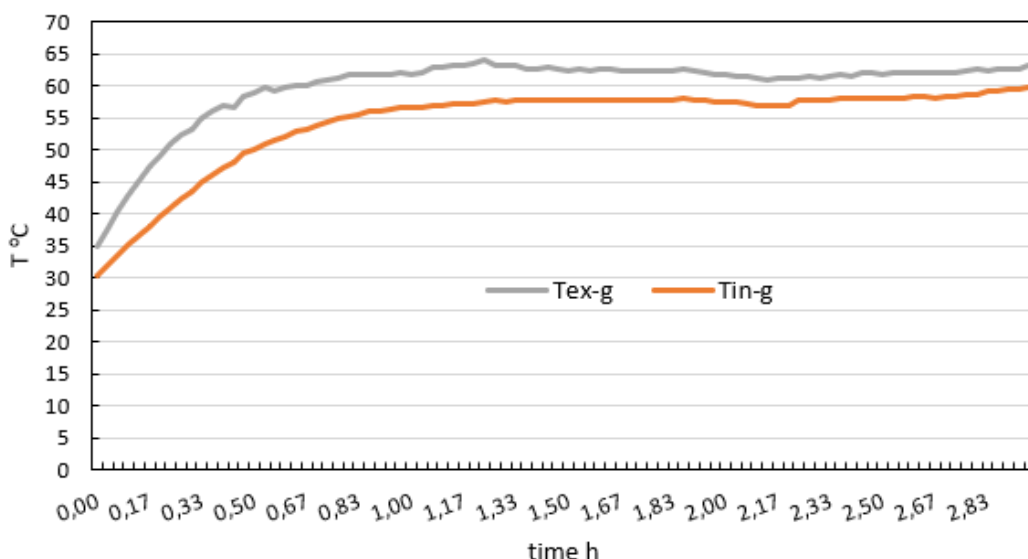


Figure 8. Internal, external temperatures for double glass windows with 9mm air gap and 1000 W/m<sup>2</sup>.

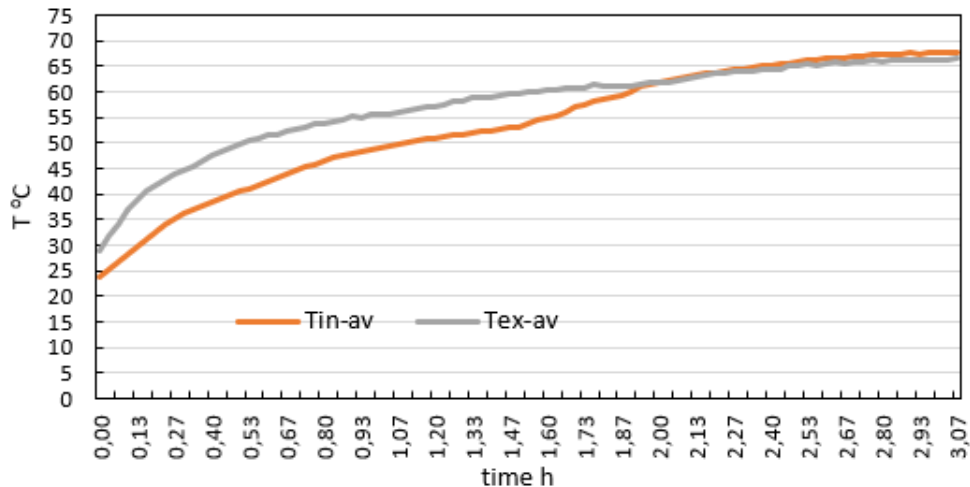


Figure 9. Internal, external and difference temperatures for 9mm air gap double glazing window with PCM (Paraffin) and  $1000 \text{ W/m}^2$ .

### Temperature Difference Analysis

Figures 10 & 11 (Temperature Differences  $\Delta T$ ):

- *Air Cavity* (Both Radiation Levels):

Exhibits minimal  $\Delta T$  ( $1.2^\circ\text{C}$  under  $500 \text{ W/m}^2$ ;  $\sim 12.5^\circ\text{C}$  under  $1000 \text{ W/m}^2$ ) due to air's low thermal conductivity ( $0.026 \text{ W/m}\cdot\text{K}$ ), enabling rapid temperature equilibration.

- *PCM Cavity*:

Sustains significantly larger  $\Delta T$  ( $\sim 13.7^\circ\text{C}$  under  $1000 \text{ W/m}^2$ ), demonstrating PCM's capacity to maintain thermal gradients through energy storage when phase change exist.

Figures 12 & 13 (Zone Temperatures):

- *Air Cavity*:

Rapid temperature spikes occur in both radiation cases, with no load-shifting capability.

- *PCM Cavity*:

for  $1000 \text{ W/m}^2$ , significant delayed by 1.5–2.67 hours and flattened temperature profiles reveal PCM's thermal buffering effect, reducing peak cooling demand.

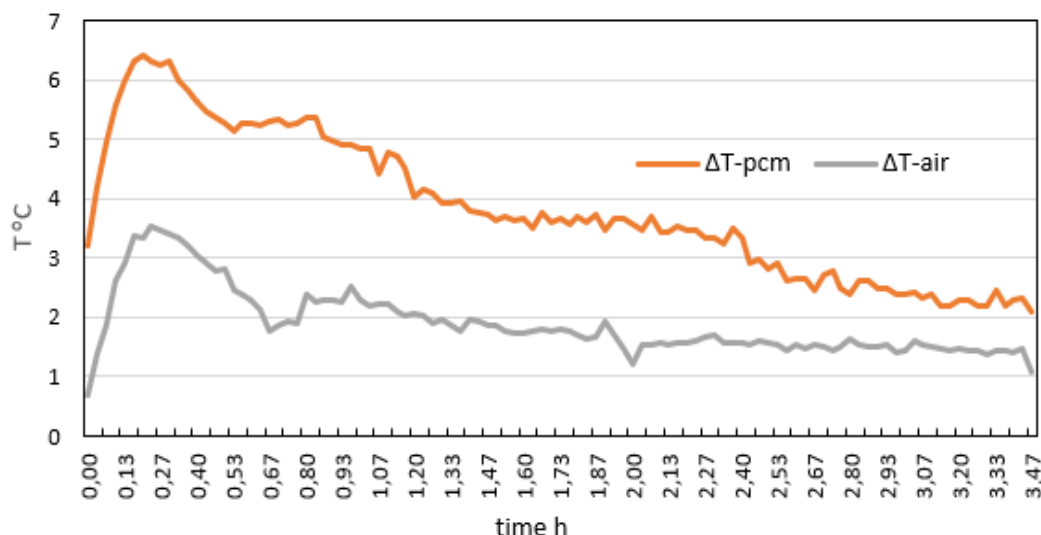


Figure 10. Temperature difference between external and internal glasses surfaces for double glass window with 9mm cavity with air and PCM under  $500 \text{ W/m}^2$ .

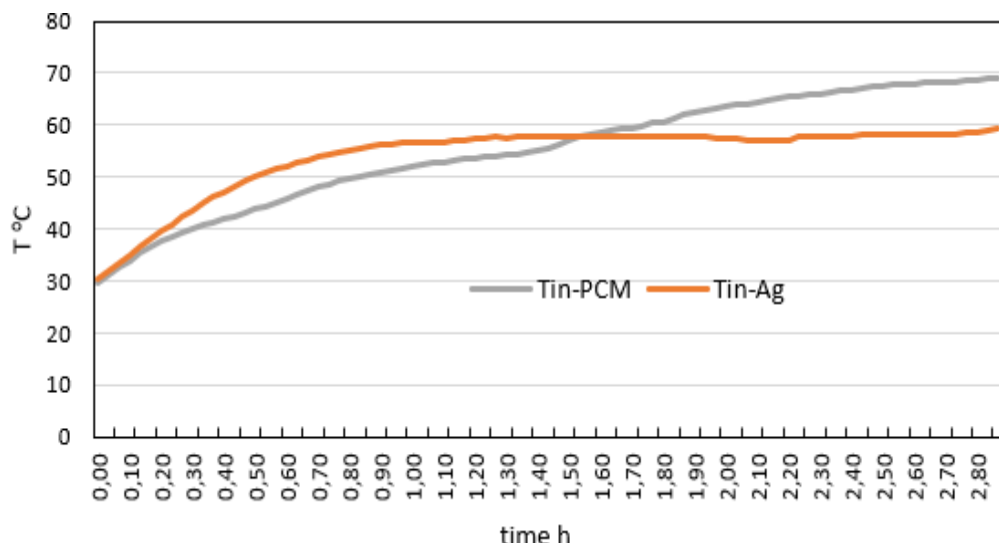


Figure 11. Internal temperature glass surfaces for double glass window with 9mm cavity with air and PCM under  $1000 \text{ W/m}^2$ .

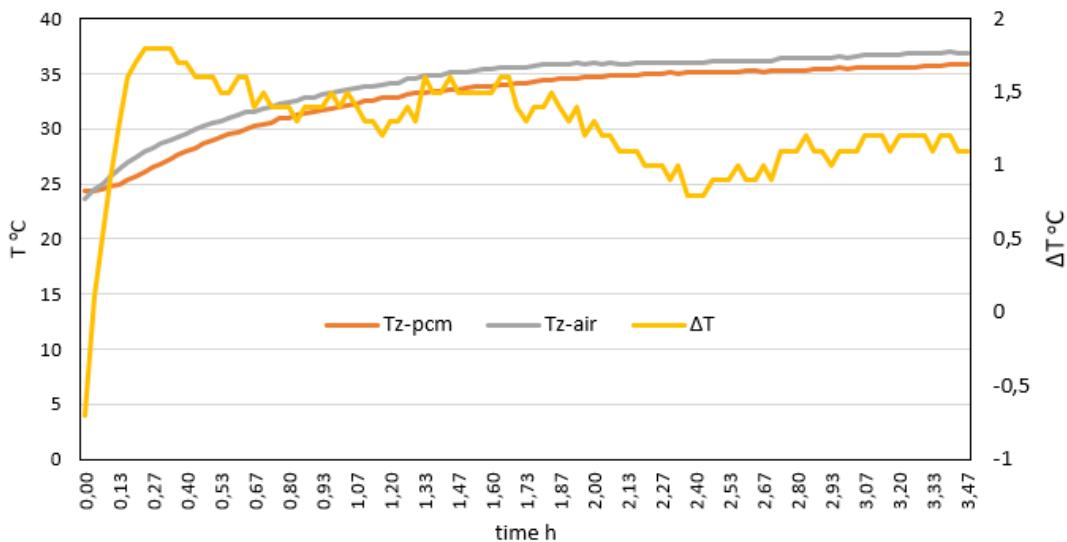


Figure 12. The zone temperatures with double glazed window with cavity 9mm with air (case1) and PCM (case2) under  $500 \text{ W/m}^2$

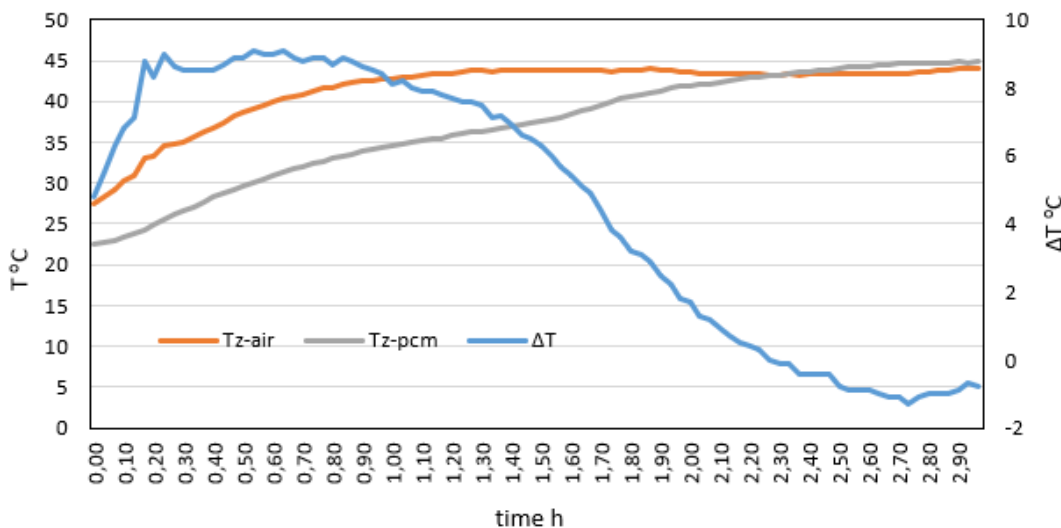


Figure 13. Zone temperature differences between double glazed window with 9mm air cavity (case1) and PCM-cavity (case2) with  $1000 \text{ W/m}^2$ .

### Internal Heat Flux Analysis

For the double glazing (air), Figure (14) are shown the heat flux under low radiation ( $500 \text{ W/m}^2$ ), while Figure (15) are shown the heat flux under radiation ( $1000 \text{ W/m}^2$ ).

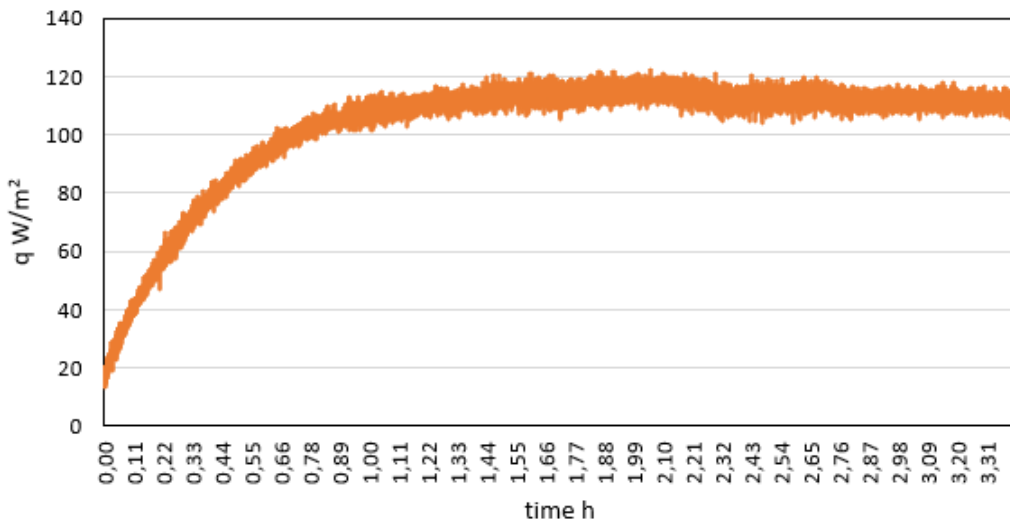


Figure 14. Heat flux inlet for double glass window with 9 mm air cavity under  $500 \text{ W/m}^2$  light intensity.

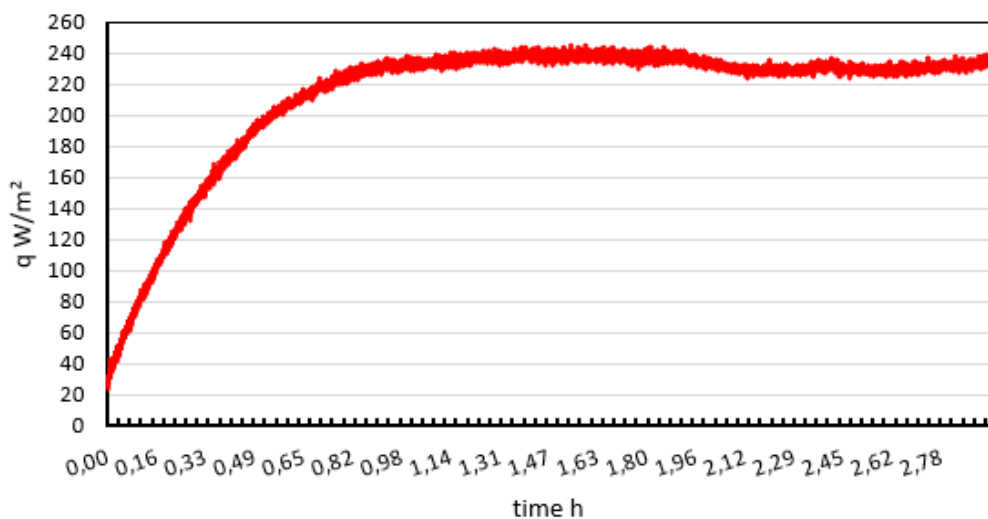


Figure 15. Input heat flux for double glass window with 9mm air cavity and  $1000 \text{ W/m}^2$  light intensity.

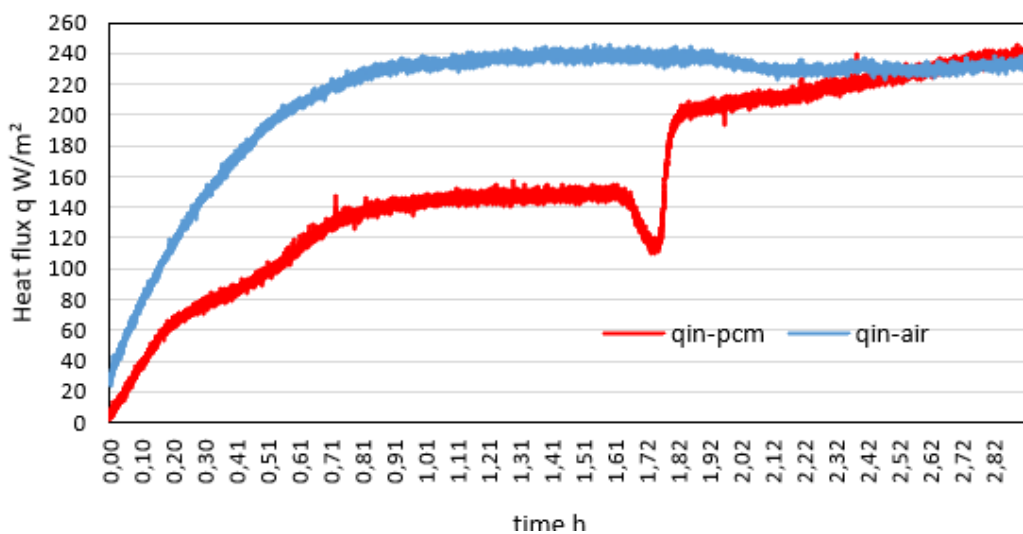


Figure 16. Internal heat flux for window with double glass-air cavity and glass-PCM cavity under  $1000 \text{ W/m}^2$

Figure 16 shows the difference between heat Flux which in case using air or Paraffin in the double glazing, window under radiation (1000 W/m<sup>2</sup>). Elevated solar radiation intensity exacerbates heat transfer through windows. PCMs mitigate this via latent heat storage, as shown under 500–1000 W/m<sup>2</sup> irradiance:

1. *Latent Heat Dominance*: PCM reduced *cumulative heat transfer* by (using equation 6) 22% (at 500 W/m<sup>2</sup>) and 35% (at 1000 W/m<sup>2</sup>) but increased *peak flux* by 15% at 500 W/m<sup>2</sup> due to solid-state conduction.
2. *Radiation-Dependent Efficacy*: The 13-percentage-point improvement at 1000 W/m<sup>2</sup> correlates with PCM activation above 56°C.
3. *Thermal Buffering*: PCM delays peak loads by 2.67 h (at 1000 W/m<sup>2</sup>) and reduces glass  $\Delta T$  by (using equation 5) 20.4%, shifting cooling demand via phase-change hysteresis.

### Implications for Building Energy Performance

The results showed that the double-glazed window model filled with phase change material (PCM) reduces heat flow by 35% under high solar radiation (1000 W/m<sup>2</sup>) compared to the same model filled with air. To assess the practical impact of this reduction, annual energy savings were calculated for a typical residential building in high solar radiation regions (for example, Baghdad/Iraq) using Baghdad's Typical Meteorological Year (TMY) data: (OpenEi)

- Heat flux reduction:  $12.88 \text{ W/m}^2 = 0.01288 \text{ kW/m}^2$  (35% of measured  $36.8 \text{ W/m}^2$  for air-filled windows).
- Effective daily radiation period ( $\geq 1000 \text{ W/m}^2$ ): 4 hours daily during peak times (10:00 AM - 2:00 PM).
- Cooling season (operation period of cooling devices): 150 days (from May to September).

Extending these remarks yields:

$$\begin{aligned} \text{Annual Savings} &= (\text{Heat Flux Reduction}) \times (\text{Daily Peak Hours}) \times (\text{Cooling Days}) \\ &= 0.01288 \text{ kW/m}^2 \times 4 \text{ h/day} \times 150 \text{ days} = 7.73 \text{ kWh/m}^2 \end{aligned}$$

Taking into account the diurnal fluctuation of radiation (assuming a weighted average of 650 W/m<sup>2</sup>), the net heat flux reduction is 22.75%, resulting in:

$$\text{Revised savings (net energy saving)} = 7.73 \text{ kWh/m}^2 \times \frac{22.75}{35} = 12.7 \text{ kWh/m}^2$$

The reduction in building cooling costs of 18-22%, due to:

- Windows contribute approximately 30% of the total cooling loads (ASHRAE, 2017).
- PCM reduces heat gain through windows by 35%.
- For buildings with a cooling intensity of 60-80 kWh/m<sup>2</sup>/year, the system achieves a saving of 21.2% of the energy consumption associated with windows.

These results are consistent with field studies in similar climates (e.g. 11-15% savings reported by (Nsaif, et al., 2023), which confirms the feasibility of applying PCM in energy-efficient buildings in areas with solar exposure higher than 2500 kWh/m<sup>2</sup>/year.

### Conclusions

The study demonstrates that double-glazed windows integrated with Phase Change Material (PCM) significantly outperform air-filled windows under high solar radiation levels ( $\geq 1000 \text{ W/m}^2$ ) when phase change activation occurs. This advantage stems from paraffin's capacity as a PCM to absorb latent heat during melting (within the 56-58°C range) and release it during solidification, thereby slowing heat transfer and stabilizing indoor temperatures. Although PCM-containing samples recorded higher absolute internal temperatures (+3.83°C at 1000 W/m<sup>2</sup>), they achieved the following results:

1. 35% reduction in cumulative heat transfer (compared to air) under 1000 W/m<sup>2</sup> radiation, attributed to latent energy buffering.
2. 20.4% reduction in glass surface thermal gradients ( $\Delta T$ ) under 1000 W/m<sup>2</sup>.
3. 2.67-hour delay in peak thermal loads under 1000 W/m<sup>2</sup>, leading to redistributed cooling demand.

Under low radiation ( $500 \text{ W/m}^2$ ), PCM remained solid, increasing heat flux by 15% due to higher conductivity ( $0.2 \text{ W/m}\cdot\text{K}$  vs. air's  $0.026 \text{ W/m}\cdot\text{K}$ ) but still reducing cumulative heat transfer by 22% through enhanced thermal mass.

This trade-off between temperature moderation and energy absorption enhances building efficiency via:

1. Peak cooling load reduction in high-radiation conditions.
2. Decreased HVAC energy intensity through load shifting.
3. Passive utilization of phase-change hysteresis for diurnal climate buffering.

Future studies should investigate long-term PCM stability under UV exposure and hybrid designs integrating low-e coatings with Nano-PCMs.

## Scientific Ethics Declaration

\* The authors declare that the scientific, ethical, and legal responsibility for the content of this article published in the EPSTEM journal belongs entirely to the authors.

\* This study does not involve any human or animal subjects and therefore did not require ethics committee approval.

## Conflict of Interest

\* The authors declare that they have no conflicts of interest.

## Funding

\* The authors received no specific funding for this research.

## Acknowledgements or Notes

\* This article will be presented as an oral presentation at the International Conference on Engineering and Advanced Technology (ICEAT) held in Selangor, Malaysia on July 23-24, 2025.

## References

Alaa Abdulhussein, M., & Hashem, A. (2021). Experimental study of the thermal behavior of perforated bricks wall integrated with PCM. *International Journal of Heat and Technology*, 39, 1917-1922.

Alharari, A. A., Khalifa, A. A. A., & Abdelhameed, A. T. (2023). Numerical analysis for the comparison of thermal performance of single and double-glazed windows in the climatic region of Libya. *International Science and Technology Journal*, 36(2).

ASHRAE. (2017). *ASHRAE handbook: Fundamentals* (SI ed.). ASHRAE.

Cieslinski, J., Boroń, P., & Fabrykiewicz, M. (2023). Stability investigation of the PCM nanocomposites. *Acta Mechanica et Automatica*, 17, 381-389.

D'Oliveira, E. J., Pereira, S. C. C., Groulx, D., & Azimov, U. (2022). Thermophysical properties of nano-enhanced phase change materials for domestic heating applications. *Journal of Energy Storage*, 46, 103794.

Filippin, C., & Larsen, S. F. (2007). Energy efficiency in buildings. In K. A. Hofman (Ed.), *Energy efficiency, recovery and storage* (pp. 223–245). Nova Science Publishers.

FluxTeq. (n.d.). *Products*. Retrieved from <https://www.fluxteq.com/products>

Gaur, M., Makonin, S., Bajic, I., & Majumdar, A. (2019). Performance evaluation of techniques for identifying abnormal energy consumption in buildings. *IEEE Access*, 7, 62721-62733

Gloriant, F., Tittelein, P., Joulin, A., & Lassue, S. (2015). Modeling a triple-glazed supply-air window. *Building and Environment*, 84, 1-9.

Goia, F., Zinzi, M., Carnielo, E., & Serra, V. (2015). Spectral and angular solar properties of a PCM-filled double glazing unit. *Energy and Buildings*, 87, 302-312.

Gosselin, J. R., & Chen, Q. (2008). A dual airflow window for indoor air quality improvement and energy conservation in buildings. *HVAC&R Research*, 14(3), 359-372.

Guo, J., & Zhang, C. (2022). Utilization of window system as exhaust air heat recovery device and its energy performance evaluation: A comparative study. *Energies*, 15(9), 3116.

Li, D., Ma, T., Liu, C., Zheng, Y., Wang, Z., & Liu, X. (2016). Thermal performance of a PCM-filled double glazing unit with different optical properties of phase change material. *Energy and Buildings*, 119, 143-152.

Liu, C., Zheng, Y., Li, D., Qi, H., & Liu, X. (2016). A model to determine thermal performance of a non-ventilated double glazing unit with PCM and experimental validation. *Procedia Engineering*, 157, 293-300.

Loba Chemie. (n.d.). *Paraffin wax pellets (56-58°C)*. Retrieved from

Lu, Y., Aldawood, F. K., Hu, W., Ma, Y., Kchaou, M., Zhang, C., Yang, X., Yang, R., Qi, Z., & Li, D. (2023). Optimization strategy for selecting the combination structure of multilayer phase change material (PCM) glazing windows under different climate zones. *Sustainability*, 15(23).

Marhoon, I., Abdulwahhab Atiyah, I., Mohammed Salih, T., & Eleiwi, M. (2024). Contribution of nanoparticles in elaborating the thermal performance of phase change materials: Up-to-date review study. *Samarra Journal of Engineering Science and Research*, 2, 91-107.

Merli, F., & Buratti, C. (2024). Properties and energy performance of wood waste sustainable panels resulting from the fabrication of innovative monolithic aerogel glazing systems. *Construction and Building Materials*, 438, 137310.

Michael, M., Favoino, F., Jin, Q., Luna-Navarro, A., & Overend, M. (2023). A systematic review and classification of glazing technologies for building façades. *Energies*, 16(14), 5357.

Nsaif, M., Baccar, M., & Jalil, J. (2023). Phase change material in glazing windows system: A review. *Engineering and Technology Journal*, 1-17.

Nsaif, M., Jalil, J., & Baccar, M. (2024). Study the thermal performance of a PCM layer-filled triple glazed window under Iraqi climate conditions. *Tikrit Journal of Engineering Sciences*, 31, 246-257.

OpenEi. (n.d.). *Open energy information, data and resources*. Retrieved from <https://openei.org/wiki/Weather>

Wang, G., Ma, Y., Zhang, S., Li, D., Hu, R., & Zhou, Y. (2023). Thermal performance of a novel double-glazed window combining PCM and solar control glass in summer. *Renewable Energy*, 219, 119363.

Zhang, G., Wang, Z., Li, D., Wu, Y., & Arici, M. (2020). Seasonal thermal performance analysis of glazed window filled with paraffin including various nanoparticles. *International Journal of Energy Research*, 44.

---

### Author(s) Information

---

**Mai AbdulKhaleq Abd-Oun**

University of Al-Qadisiyah, Al-Diwaniyah,  
Iraq  
Contact email: [may.abdalkhaliq@qu.edu.iq](mailto:may.abdalkhaliq@qu.edu.iq)

**Alaa Liaq Hashem**

University of Al-Qadisiyah, Al-Diwaniyah,  
Iraq

**Ahmed AbdelKadhem Majhool**

University of Al-Qadisiyah, Al-Diwaniyah,  
Iraq

---

**To cite this article:**

Abd-Oun, M. A., Hashem, A.L., & Majhool, A. A. (2025). Experimental investigation of energy performance in double-glazed windows utilizing air and phase change materials. *The Eurasia Proceedings of Science, Technology, Engineering and Mathematics (EPSTEM)*, 37, 359-373.